

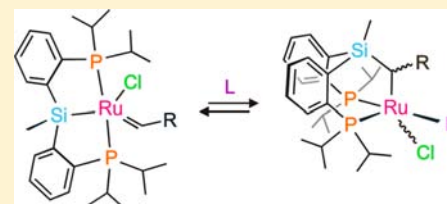
Reversible Insertion of Carbenes into Ruthenium–Silicon Bonds

María J. Bernal, Olga Torres, Marta Martín,* and Eduardo Sola*

Instituto de Síntesis Química y Catálisis Homogénea (ISQCH), CSIC-Universidad de Zaragoza, E-50009 Zaragoza, Spain

S Supporting Information

ABSTRACT: The five-coordinate carbene complexes $[\text{Ru}\{\kappa\text{P},\text{P},\text{Si}-\text{Si}(\text{Me})(\text{C}_6\text{H}_4-2\text{-PiPr}_2)_2\}\text{Cl}(\text{=CHR})]$ (**2**, R = Ph; **3**, R = SiMe₃), analogues of the Grubbs catalyst, were prepared from the dimer $[\text{Ru}(\mu\text{-Cl})\{\kappa\text{P},\text{P},\text{Si}-\text{Si}(\text{Me})(\text{C}_6\text{H}_4-2\text{-PiPr}_2)_2\}]_2$ (**1**) and the corresponding diazoalkane N₂CHR. The particular structural features that result from the presence of a strongly trans directing silyl group at the pincer ligand of these complexes are discussed on the basis of NMR information and the crystal structure of the vinylidene analogue $[\text{Ru}\{\kappa\text{P},\text{P},\text{Si}-\text{Si}(\text{Me})(\text{C}_6\text{H}_4-2\text{-PiPr}_2)_2\}\text{Cl}(\text{=C=CHPh})]$ (**4**), which was also obtained from **1** and phenylacetylene. The reactions of **3** with reagents such as P(OMe)₃, CO, NCMe, and K(acac) illustrate that the first response of these carbene complexes to an increase of the coordination number around ruthenium is the insertion of the carbene ligand into the Ru–Si bond. These reactions also indicate that the insertion process is reversible and allows typical transformations of carbene ligands such as C–H functionalizations via carbene insertion (in the acac ligand) or the formation of ketene from CO. In addition, the reactions of **3** with terminal alkynes such as phenylacetylene or 3,3-dimethyl-1-butyne show that the inserted carbenes can also undergo reactions typical of metal-bound alkyls such as alkyne insertion and C–H reductive elimination.



INTRODUCTION

As our mechanistic understanding of coordination and organometallic chemistry increases, we are able to recognize more reactions in which the ligands play a role beyond the mere stereoelectronic influence. Thus, it is increasingly common to find in the chemical literature labels such as “noninnocent”,¹ “cooperating”,² or bifunctional,³ to highlight certain properties of some ligands that render them particularly suitable or even essential for transformations occurring at the coordination sphere of metal complexes. Sometimes, the origin of such ligand contributions is an electronic reorganization: a valence tautomerism or resonance.^{1,4} In other cases, it is a reversible bond cleavage or formation that happens in the presence of reagents.^{2,3,5,6} Several biochemically relevant systems exploit examples of the first type,⁷ while the latter is at the heart of highly efficient catalytic cycles⁸ and valuable stoichiometric reaction sequences.⁹ This work features a recourse of the latter type for pincer ligands that contain a silyl donor group ($\kappa\text{P},\text{P},\text{Si}$), which consists of a reversible insertion of carbenes into the metal–silicon bond.

Our interest in these types of pincers was originally due to their capability of controlling the coordination geometry of unsaturated metal complexes via the large trans influence of the silyl group.^{10,11} We intended to exploit this property to shape analogues of the Grubbs catalyst with the vacant coordination site cis to the carbene ligand.¹² In our hypothesis, such five-coordinate ruthenium complexes could work as olefin metathesis catalysts without the need for preactivating via ligand dissociation,¹³ thus potentially leading to more robust, compatible, and reusable catalysts. The following pages show that even though the target nonisostructural analogues of the Grubbs catalyst are readily accessible, their behavior is

dominated by the title reaction and do not work as olefin metathesis catalysts.

RESULTS AND DISCUSSION

Grubbs Catalyst Analogues Based on a $\kappa\text{P},\text{P},\text{Si}$ Pincer.

The dimer $[\text{Ru}(\mu\text{-Cl})\{\kappa\text{P},\text{P},\text{Si}-\text{Si}(\text{Me})(\text{C}_6\text{H}_4-2\text{-PiPr}_2)_2\}]_2$ (**1**) turned out to be a suitable precursor for the preparation of carbene complexes. It was obtained from the reaction of $[\text{Ru}(\mu\text{-Cl})_2(\text{cod})]_n$ with the silane $\text{HSi}(\text{Me})(\text{C}_6\text{H}_4-2\text{-PiPr}_2)_2$ in the presence of triethylamine. The structure of **1** determined by X-ray crystallography, virtually C₂ symmetric (Figure 1), is similar to that reported by Tobish, Turculet, et al. for the analogous complex with cyclohexyl instead of isopropyl groups.¹⁴ Also similarly to this precedent, the NMR spectra of **1** in solution at room temperature indicate an average higher symmetry, by showing for example a single broad resonance in the ³¹P{¹H} spectrum corresponding to the four phosphorus atoms.

Compound **1** was found to react with diazoalkanes such as phenyldiazomethane and trimethylsilyldiazomethane, releasing N₂ and forming the carbene complexes $[\text{Ru}\{\kappa\text{P},\text{P},\text{Si}-\text{Si}(\text{Me})(\text{C}_6\text{H}_4-2\text{-PiPr}_2)_2\}\text{Cl}(\text{=CHR})]$ (**2**, R = Ph; **3**, R = SiMe₃), respectively (Scheme 1). The commercial ethyl diazoacetate, however, did not react cleanly under the same conditions, thus showing that this synthetic method is not applicable to any diazoalkane reagent. Actually, only the formation of **3** seems to be clean and selective, as the reaction leading to compound **2** always gave rise to variable amounts of still unidentified byproducts.

Received: October 22, 2013

Published: December 1, 2013

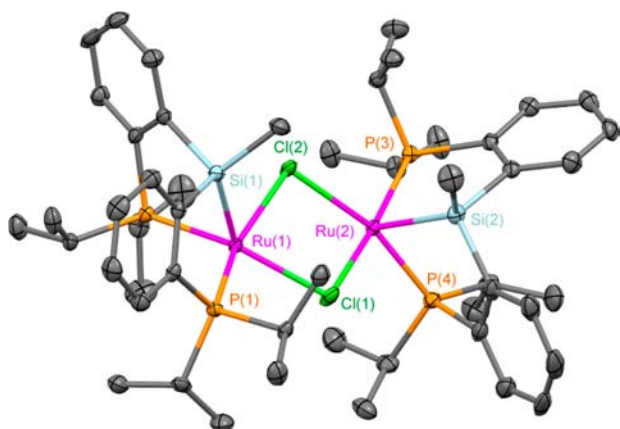
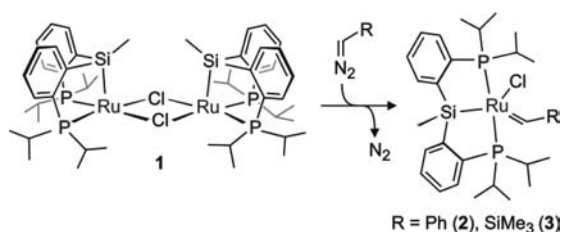


Figure 1. Crystal structure of complex **1** at the 50% probability level. The hydrogen atoms are omitted for clarity. For bond distances and angles see the Supporting Information.

Scheme 1



Complexes **2** and **3** show NMR spectra consistent with equivalent and mutually trans $\kappa P, P, Si$ groups, indicating a change of the coordination mode of the $\kappa P, P, Si$ ligand from *fac* (in **1**) to *mer*. Accordingly, the carbene ligand CHs give rise to characteristic triplet signals in both the 1H and $^{13}C\{^1H\}$ NMR spectra: at δ 12.51 ($J_{HP} = 6.2$) and 264.69 ($J_{CP} = 3.1$), respectively, for **2** and at δ 12.44 ($J_{HP} = 1.8$) and 274.95 ($J_{CP} = 4.9$) for **3**.

Although, so far, we have not been able to grow good crystals for any of these carbene complexes, their likely structural features can be discussed on the basis of the X-ray diffraction structure of the analogous vinylidene compound $[Ru\{\kappa P, P, Si-Si(Me)(C_6H_4-2-PiPr_2)_2\}Cl(=C=CHPh)]$ (**4**; Figure 2). This derivative was also prepared from precursor **1** by reaction with

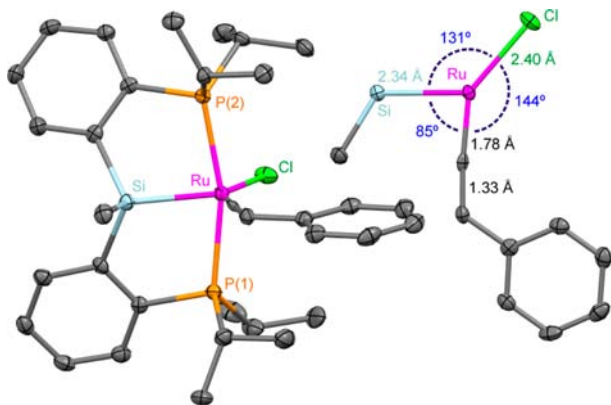
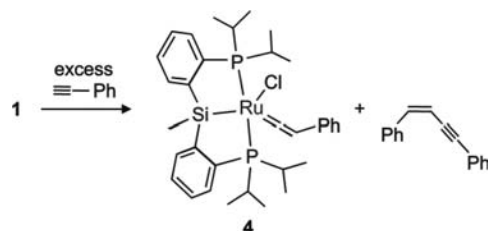


Figure 2. (left) Crystal structure of **4** (50% probability level) and (right) structural details of the equatorial plane of the complex. The hydrogen atoms are omitted for clarity. For other bond distances and angles see the Supporting Information.

phenylacetylene at room temperature (Scheme 2). The synthesis required several equivalents of the alkyne reagent,

Scheme 2



as **4** was formed together with the product of phenylacetylene dimerization (*Z*)-1,4-diphenyl-1-buten-3-yne. Similar selective dimerization processes have already been observed for the parent vinylidene complexes $[RuCl_2(=C=CHPh)(PR_3)_2]$ (R = *i*Pr, Cy) as catalysts.¹⁵

Figure 2 details the angles in the equatorial plane of the five-coordinate complex **4** to stress the differences with those found in the aforementioned vinylidene analogues of the Grubbs catalyst $[RuCl_2(=C=CHPh)(PR_3)_2]$. In the latter, the vacant coordination site clearly sits *trans* to the strongly σ -donor vinylidene ligand, with angles between the chlorides of 161° (R = *i*Pr),¹⁶ and 158° (R = Cy).^{16,17} In contrast, the silyl function of the $\kappa P, P, Si$ pincer of **4** seems capable of opening up the *trans* angle to 144° even in the presence of the vinylidene, whose *trans* angle closes to 131° . In favor of attributing these differences mainly to a competition among the *trans* influences of the equatorial ligands, the related derivative $[RuCl(NO)(=C=CHPh)(PPh_3)_2]$ also shows the widest angle (139°) *trans* to the *trans*-directing bent nitrosyl ligand,¹⁸ while that *trans* to vinylidene is just 113° .¹⁹

Among the various possible isomers for the products of the above reactions, those represented in Schemes 1 and 2 are the major isomers (**2** and **3**) or the only species detectable by NMR (**4**). In this isomer, the carbene or vinylidene ligand occupies the (less hindered) coordination position *syn* to the methyl at silicon, while the substituent at the carbene or vinylidene avoids the vicinity of this methyl. This is inferred, for all complexes, from the observation of NOE between the 1H NMR signals corresponding to the SiMe and the carbene or vinylidene hydrogen and is confirmed by the crystal structure of **4**. Such a product selectivity suggests that the $\kappa P, P, Si$ pincer provides by itself a congested coordination environment. Furthermore, other NMR parameters suggest that the pincer can adapt its coordination angles to accommodate bulky equatorial ligands. This is illustrated in Figure 3 by means of two of the $^{13}C\{^1H\}$ NMR signals that are sensitive to the magnitude of the $J_{PP'}$ coupling constant, because they correspond to carbons of the pincer backbone for which the two chemically equivalent ^{31}P nuclei are magnetically inequivalent. The signals of complex **4**, whose crystal structure indicates a P–Ru–P angle of 165° , are virtual triplets characteristic of strongly coupled phosphorus. This is also the case for the phenyl-substituted carbene **2** but not for the trimethylsilyl-substituted derivative **3**, whose signals show features halfway between the virtual triplet and those typical of weakly coupled phosphorus. The latter are exemplified in the figure by the signals of complex **1**, the structure of which shows P–Ru–P angles of 95 and 105° and whose 303 K NMR spectrum indicates an averaged $J_{PP'}$ coupling constant of about

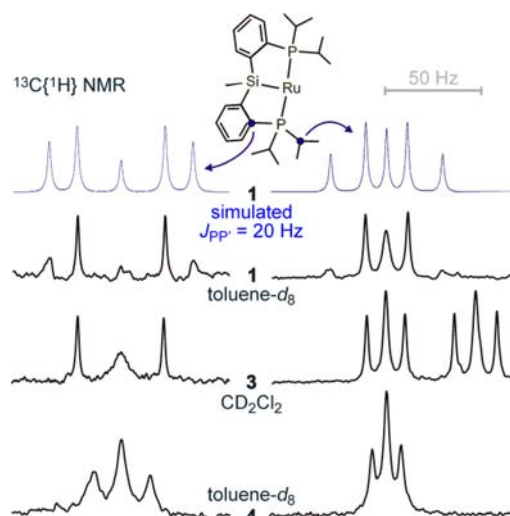


Figure 3. Examples of $^{13}\text{C}\{^1\text{H}\}$ NMR signals corresponding to A nuclei in AXX' spin systems ($X = ^{31}\text{P}$) for complexes **1**, **3**, and **4**.

20 Hz. Even though the signal to noise ratio of the $^{13}\text{C}\{^1\text{H}\}$ NMR spectrum of **3** does not allow observation of those side lines of the AXX' spin system that make possible the evaluation of the $J_{\text{PP}'}$ constant, the shape of these signals can be considered diagnostic of a distortion of the *mer* pincer toward a *fac* coordination.

Carbene Insertion. The possible catalytic activity of the unsaturated carbene complexes **2** and **3** in olefin metathesis was investigated through reactions and protocols previously proposed in the literature as a standard system of characterization.²⁰ None of these experiments gave positive results. The only noticeable observation was the slow isomerization of substrates such as 1,5-cyclooctadiene, diethyldiallyl malonate, allylbenzene, and *cis*-1,4-diacetoxy-2-butene, which was not further investigated. The in situ NMR examination of reactions with excess ethylene also did not produce noticeable results. However, in contrast to the inertness suggested by these initial experiments, many reagents other than olefins were observed to react with these five-coordinate complexes. The three selected reactions of complex **3** depicted in Scheme 3 support the description and discussion of the elementary process that was repeatedly observed upon ligand or reagent coordination: the insertion of the carbene ligand into the Ru–Si bond.

After addition of 1 equiv of trimethyl phosphite, the solutions of **3** in acetone- d_6 showed broadened room-temperature ^1H and $^{31}\text{P}\{^1\text{H}\}$ NMR spectra (Figure 4). The spectra at low temperature revealed the formation of two new products which, according to their sets of J_{PP} coupling constants (major product, 416.9, 78.3, and 17.3 Hz; minor product, 236.4, 42.3, and 26.3 Hz), show *mer* arrangements of three inequivalent phosphorus atoms. In view of the typical values for ^{31}P chemical shifts, the major product should have two mutually *cis* $\text{P}i\text{Pr}_2$ groups, while in the minor product these groups seem to be *trans*. The major product could be identified from its NMR signals as complex **5** (Scheme 3), although due to the weakness of the ^1H NMR NOE effects at the low temperatures required to observe narrow spectra, some details of its stereochemistry remain unknown. Notably, its $^{13}\text{C}\{^1\text{H}\}$ NMR spectrum at 193 K does not show any signal attributable to a carbene ligand. Instead, an apparent quartet at very high field ($\delta = -42.60$, CH) with J_{CP} coupling constants of about 8 Hz can be attributed to a new Ru–alkyl moiety *cis* to three phosphorus atoms. A second

Scheme 3

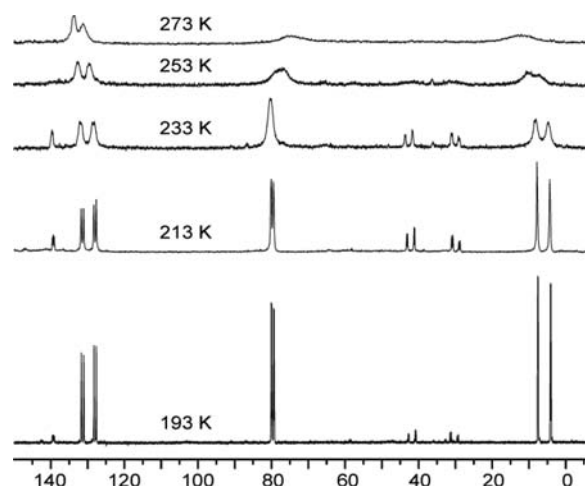
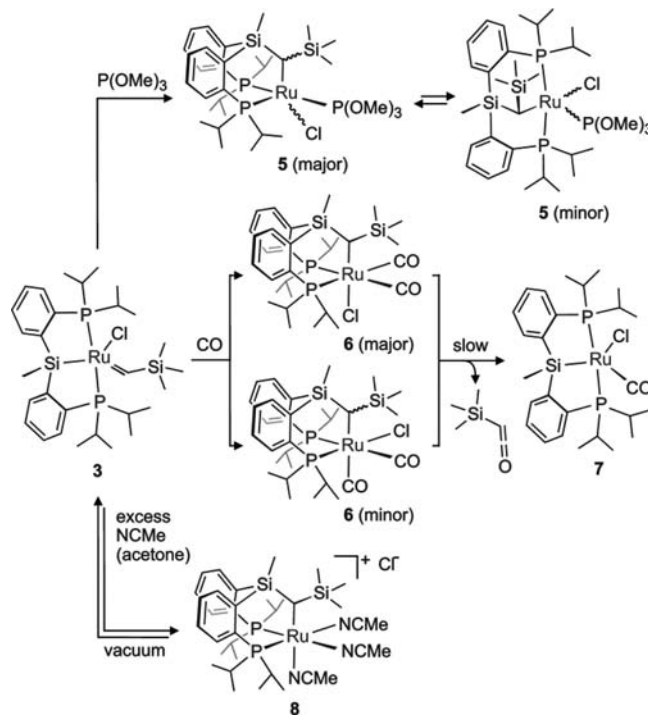


Figure 4. $^{31}\text{P}\{^1\text{H}\}$ NMR spectra of the reaction of **3** with 1 equiv of $\text{P}(\text{OMe})_3$ in acetone- d_6 at various temperatures.

significant change in the NMR spectra upon reaction is the pronounced shift of the $^{29}\text{Si}\{^1\text{H}\}$ signal corresponding to the silicon of the pincer (Figure 5), which moves from δ 50.72 (t, $J_{\text{SiP}} = 11.7$ Hz) to δ -9.76 (dd, $J_{\text{SiP}} = 21.1$ and 6.8 Hz). A common explanation for these two NMR features would imply an insertion of the carbene ligand into the Ru–Si bond. Such a process generates a chiral center and therefore inequivalent pincer phosphorus atoms, whatever the ligand arrangement. Taking this into account and in view of the $^{29}\text{Si}\{^1\text{H}\}$ NMR signals observed for the minor product of this reaction (Figure 5), this second complex should also contain a $\kappa\text{C},\text{P},\text{P}$ pincer generated via carbene insertion, but coordinated in a *mer* fashion. Furthermore, the VT evolution of the NMR spectra (^{31}P in Figure 4) suggests that the spectral broadening can be attributed to the exchange between both isomers of **5** in equilibrium.

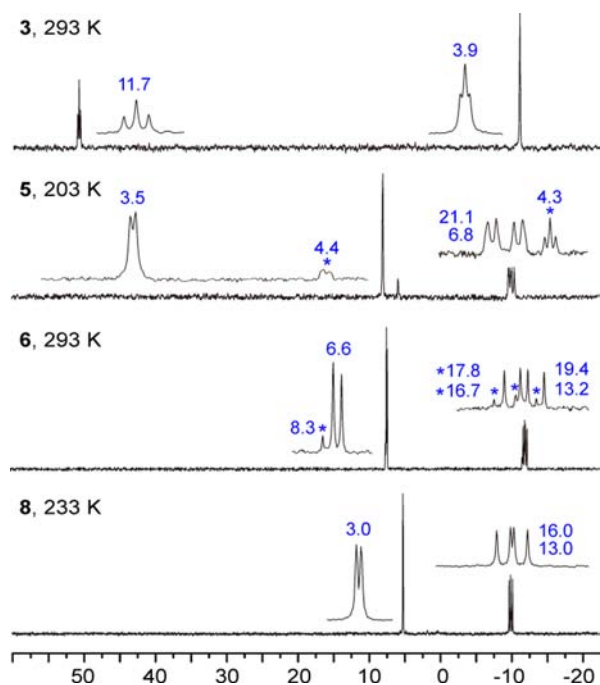


Figure 5. $^{29}\text{Si}\{^1\text{H}\}$ NMR spectra of **3** and the products of its reactions with $\text{P}(\text{OMe})_3$ (**5**), excess CO (**6**) and excess NCMe (**8**). J_{SiP} coupling constants are shown in blue. Asterisks denote signals and constants corresponding to the minor products.

The second example in Scheme 3, the reaction of **3** with CO, was monitored by NMR in CD_2Cl_2 solution. After bubbling of CO and subsequent removal of the excess CO with bubbling argon, a mixture of two new complexes was again observed. The NMR spectra of both products display the aforementioned features diagnostic of the carbene insertion: inequivalent phosphorus atoms, negative chemical shifts for the $^{29}\text{Si}\{^1\text{H}\}$ NMR signals of the pincer, and high-field CH multiplets in the $^{13}\text{C}\{^1\text{H}\}$ NMR spectrum (apparent triplets in this case). The major product (ca. 90%), complex **6** in Scheme 3, shows two CO $^{13}\text{C}\{^1\text{H}\}$ NMR signals indicative of ligands trans to phosphorus: doublets of doublets at δ 199.02 and 198.09 with J_{CP} coupling constants of 77.2, 17.2 Hz and 74.7, 20.2 Hz, respectively. Also in view of its CO $^{13}\text{C}\{^1\text{H}\}$ NMR signals, the minor product of this reaction should be an isomer of **6** with the chloride trans to phosphorus, although the spectra do not allow us to distinguish between the two possibilities.

Complex **6** was found to slowly transform (days at room temperature) into the five-coordinate complex $[\text{Ru}\{\kappa\text{P},\text{P},\text{Si}-\text{Si}(\text{Me})(\text{C}_6\text{H}_4-2-\text{PiPr}_2)_2\}\text{Cl}(\text{CO})]$ (**7**) and trimethylsilylketene. The latter was identified in the reaction mixture by means of its reported ^1H , $^{13}\text{C}\{^1\text{H}\}$, and $^{29}\text{Si}\{^1\text{H}\}$ NMR signals.²¹ This reactive compound was formed just as a transient species, disappearing to give products that could not be identified. Complex **7** was formed as a single isomer displaying a *syn* relative orientation of the CO ligand and the methyl at silicon. This compound could also be prepared by alternative methods such as the reaction of precursor $[\text{RuHCl}(\text{CO})(\text{PPh}_3)_3]$ with the silane $\text{HSi}(\text{Me})(\text{C}_6\text{H}_4-2-\text{PiPr}_2)_2$ or, more simply, by addition of a drop of ethanol during the synthesis of **1**. The crystal structure of **7** can be found in the Supporting Information. Its most noticeable feature is an angle trans to silicon of 178° , which supports the structural arguments based on trans influences given in the previous section. The possible

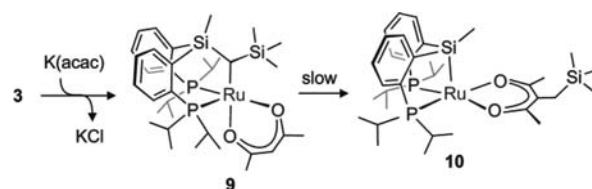
reaction of **7** with trimethylsilyldiazomethane was investigated because it could enable a catalytic synthesis of the ketene.²² However, the only new products detected by NMR in this reaction were those of carbene dimerization.

The observed evolution of **6** strongly suggests that the process of carbene insertion into the Ru–Si bond is reversible. A much clearer evidence of that was obtained from the last reaction of Scheme 3, in which the acetonitrile provoked not only the carbene insertion but also the displacement of the chloride outside the coordination sphere of the metal. The single product of this reaction, the cationic complex **8**, showed broadened NMR spectra above 240 K due to facile acetonitrile dissociation. At low temperature, the ^1H , $^{13}\text{C}\{^1\text{H}\}$, and $^{29}\text{Si}\{^1\text{H}\}$ (Figure 5) NMR spectra were fully consistent with the proposed structure. It is worth noting that when the solutions of **8** were dried in vacuo and the residue was redissolved, the NMR spectra indicated the quantitative regeneration of the carbene precursor **3**. In fact, this represented a difficulty in isolating **8** as a pure solid, which was overcome by removing the chloride from the solution with silver triflate, thus isolating **8** as its triflate salt.

Although insertion reactions of metal-bound carbenes are relatively common,^{23,24} the reactions of Scheme 3 represent, to the best of our knowledge, the first examples of such an insertion into a metal–silicon bond. Furthermore, reversible migratory insertions of carbenes such as these are rare.^{25,26} Perhaps the closest precedent for this reaction can be found in the treatment of the iridium(I) complex $[\text{Ir}\{\kappa\text{N},\text{P},\text{P}-\text{N}(\text{C}_6\text{H}_3-4-\text{Me}-2-\text{PiPr}_2)_2\}(\text{=CHO}t\text{Bu})]$ with excess CO, which causes the migratory insertion of the alkoxy carbene into the Ir–N bond of the amidophosphine pincer.²⁶ Such a process was also proposed to be reversible on the basis of the product thermal evolution, which resembles that of **6**. On the other hand, the involvement of the silicon atom of $\kappa\text{P},\text{P},\text{Si}$ pincers in processes of bond cleavage and formation has been frequently observed,^{27–29} a fact suggesting that such pincers are less inert than their $\kappa\text{C},\text{P},\text{P}$ or $\kappa\text{N},\text{P},\text{P}$ counterparts.³⁰ In particular, oxo groups and hydroxo ligands have been reported to insert respectively into Ru–Si²⁹ and Ir–Si²⁸ bonds of complexes with $\kappa\text{P},\text{P},\text{Si}$ pincers. Moreover, the reversible formation of a Si–C bond by reductive elimination might be involved in the unusual hydrocarboxylation of allenes with CO_2 catalyzed by a palladium $\kappa\text{P},\text{P},\text{Si}$ complex.³¹

X-ray diffraction confirmation of the carbene migratory insertion and further evidence of its reversibility were obtained from the reaction sequence of Scheme 4: initiated by a

Scheme 4



substitution of the chloride ligand by acetylacetonate (acac). As in the previous examples, this reaction was expected to increase the coordination number of the complex, thus triggering carbene migration.

The structure of the expected reaction product, complex **9**, is shown in Figure 6. It can be described as square pyramidal, with the vacant site trans to one of the phosphorus atoms of the new

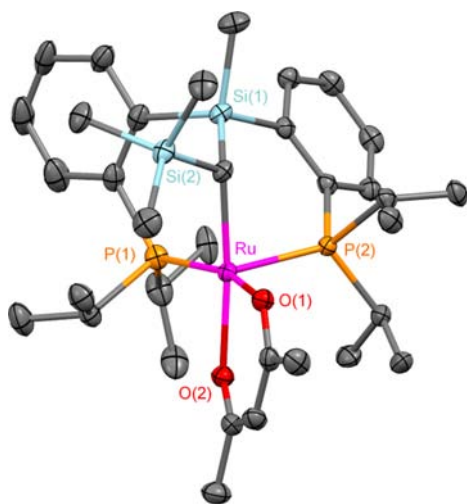


Figure 6. Crystal structure of complex **9** at the 50% probability level. The hydrogen atoms are omitted for clarity. For bond distances and angles see the Supporting Information.

fac $\kappa C, P, P$ pincer generated after carbene insertion ($P-Ru-P$ angle 104°). Although from just a consideration of trans influences this is not the most likely ligand arrangement, it seems to be the one sterically favored, as it gives more space to accommodate the bulky $SiMe_3$ group. In any case, the trans influences of the alkyl and phosphorus arms of the pincer are not that different, as inferred from the two $Ru-O$ distances of the acac ligand: 2.1385(13) Å trans to C and 2.0960(13) Å trans to P. In line with these considerations, it should be mentioned that the room-temperature NMR spectra of **9** are inconsistent with the solid-state structure, since both the 1H and $^{13}C\{^1H\}$ NMR signals corresponding to the acac indicate a symmetry element that relates the halves of the ligand. The spectra at low temperature, however, show the decoalescence of each NMR signal into two signals with the approximate relative integration 3:1 (in toluene- d_8). Then, the structure of **9** shown in Figure 6 should be in equilibrium with a second coordination isomer of similar energy, whose fast exchange on the NMR time scale with **9** averages the acac signals but not those of the $\kappa C, P, P$ pincer.

Complex **9** was observed to evolve in solution into a new product, **10**. The reaction took several days at room temperature but just a few hours in toluene at 363 K. The NMR spectra of **10** indicate a symmetric structure with equivalent ^{31}P nuclei: a feature by itself demonstrative of the reversal of the carbene insertion. Consistently, the $^{29}Si\{^1H\}$ NMR spectrum of the compound recovers the low-field signal characteristic of the pincer's $\kappa P, P, Si$ coordination: in this case a triplet at δ 69.37 with a J_{SiP} coupling constant of 19.0 Hz. The NMR spectra also confirm that the $SiMe_3$ group remains at the complex, although the $^{13}C\{^1H\}$ NMR spectrum does not show any CH signal attributable to a Ru-bound alkyl or carbene ligand. Instead, the disappearance of the acac CH and the presence of a new methylene group is evident from the 1H and $^{13}C\{^1H\}$ NMR spectra and their correlation experiments. All of these NMR features point to the structure of **10** shown in Scheme 4. This proposal is further supported by the similarity between the NMR spectra of **10** and those recorded for the closely related complex $[Ru\{\kappa P, P, Si-Si(Me)(C_6H_4-2-PiPr_2)_2\}-(acac)]$ (**11**), which was prepared for this purpose from **1** and $K(acac)$. The similarities between **10** and **11** include the shape

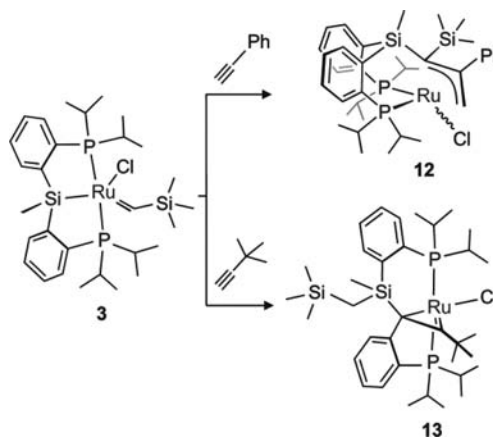
of the $^{13}C\{^1H\}$ NMR signals of the pincer backbone that are sensitive to the magnitude of the J_{PP} coupling constant (see Figure 3 and accompanying discussion), which are also similar to those of **1**, thereby indicating a *fac* coordination mode of the pincer.

Together, Schemes 1 and 4 compose a reaction sequence for acac functionalization via insertion of the carbene into a C–H bond.³² These types of functionalizations are known to be catalyzed by a variety of transition-metal complexes, especially of rhodium and coinage metals.³³ Ruthenium carbenes, however, are thought to be too unreactive for such functionalizations, as only a few exceptional examples of intramolecular reactions have been reported.³⁴ In the present case, carbene insertion into the Ru–Si bond should certainly contribute to accommodate the anionic substrate in the coordination sphere of ruthenium and might be behind the success of the process.

Further Transformations of the Inserted Carbene.

None of the aforementioned complexes featuring inserted carbenes was found to be stable in solution for long periods, although, with the exception of **6** and **9**, their evolutions turned out to be too unselective and could not be understood. Yet, the acac functionalization leading to **10** (Scheme 4) and the release of ketene from **6** (Scheme 3) demonstrate that the “masked carbenes” of these complexes remain useful for new bond formations via migratory deinsertion from the silyl-substituted metal alkyls. Nevertheless, carbene deinsertion is not the only option for these alkyls, as inferred from the two reactions between **3** and terminal alkynes shown in Scheme 5.

Scheme 5



The reaction of **3** with phenylacetylene at room temperature was complete in a few minutes, giving complex **12** together with traces of the alkyne dimerization product (*Z*)-1,4-diphenyl-1-buten-3-yne. The 1H , $^{13}C\{^1H\}$, and $^{29}Si\{^1H\}$ NMR spectra of **12** display many similarities with those of the carbene insertion products described above, although the characteristic $^{13}C\{^1H\}$ NMR high-field signal corresponding to the Ru-bound carbon is now a CH_2 instead of a CH (a doublet at δ –19.59 with a J_{CP} coupling constant of 6.8 Hz). This signal correlates in the $^1H, ^{13}C$ hsqc NMR spectrum with those of two inequivalent hydrogens: a doublet at δ –0.02 showing a J_{HH} coupling constant of 9.0 Hz and a multiplet at δ –0.34 which additionally shows two J_{HP} coupling constants of 11.5 and 2.7 Hz. In addition to the signals from carbons of the former $\kappa P, P, Si$ ligand skeleton and a phenyl ring (broad), the $^{13}C\{^1H\}$

NMR spectrum shows two resonances corresponding to quaternary carbons at δ 185.13 (dd, $J_{CP} = 17.6$ and 6.7 Hz) and 151.46 (dd, both $J_{CP} = 1.8$ Hz). These latter signals, together with that at high field, suggest the presence of a η^3 -allyl ligand, as shown in the proposed structure of **12** (Scheme 5). In favor of this proposal, the ^1H NMR nOesy spectrum indicates the proximity of the SiMe and SiMe₃ groups, while the ^1H , ^{13}C NMR hmbc correlation reveals long-range couplings between both of these groups and the CH₂. Furthermore, other potential ways of combining a carbene and an alkyne in the coordination sphere of the metal³⁵ can be discarded, because they would lead to either highly unsaturated complexes or compounds containing both intact $\kappa P,P,Si$ pincers and ligands with NMR-evident carbenoid quaternary carbons. Moreover, the most plausible pathway toward **12** from **3** and phenylacetylene is compatible with the literature results and the ease of the reaction. Assuming that, as shown in the previous pages, the alkyne coordination to ruthenium causes carbene insertion into the Ru–Si bond, the formation of **12** would consist of a further insertion of the alkyne in the Ru–alkyl moiety³⁶ followed by a 1,3-hydrogen shift, transforming the resulting alkenyl ligand into an allyl.³⁷

The second example of Scheme 5, the reaction between **3** and 3,3-dimethyl-1-butyne to form complex **13**, is much more elaborate than the previous example and, consistently, was observed to be much slower, taking several hours in dichloromethane solution at room temperature. Our monitoring of the transformation by NMR indicated that no intermediate accumulates up to concentrations allowing identification. The structure of **13** (Figure 7) meets several

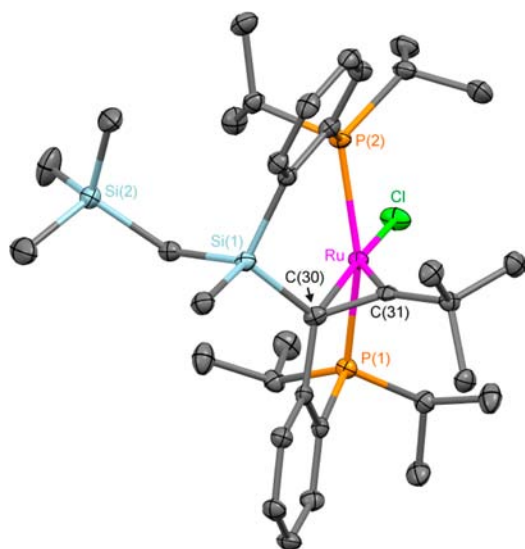


Figure 7. Crystal structure of complex **13** at the 50% probability level. The hydrogen atoms are omitted for clarity. For bond distances and angles see the Supporting Information.

notable features. It contains a new pincer ligand with an alkenyl arm that coordinates in an η^2 fashion, forming a 1-ruthenacyclopropene. This type of alkenyl coordination has been previously observed in complexes of Mo, W, Re, and Os³⁸ but not of Ru, in spite of the fact that it has been proposed to rationalize the stereochemical outcome of several transformations catalyzed by complexes of this metal.^{39,40} One such transformation is the *anti* addition of silanes to alkynes, in which the possible participation of η^2 -alkenyl intermediates

closely related to **13** has been discussed in depth.⁴⁰ The bond distances within the ruthenacyclopropene ring are consistent with the expected presence of a Ru–C double bond,³⁸ Ru–C(31) = 1.832(2) Å, Ru–C(30) = 2.183(2) Å, and C(30)–C(31) = 1.431(3) Å, and so are the $^{13}\text{C}\{^1\text{H}\}$ NMR signals corresponding to the alkenyl carbons, an apparent triplet at δ 330.45 ($J_{CP} = 5.9$ Hz) and a singlet at δ 53.81.

The structure of **13** again suggests a reaction pathway initiated by alkyne coordination and carbene insertion into the Ru–Si bond, although the presence of the CH₂Si(Me)₃ substituent at the silicon of the former pincer seems to indicate that in this example the C–H activation of the alkyne is preferred over its insertion into the Ru–C bond. The formation of **13** also entails the very unusual insertion of a putative alkynyl ligand into a Si–C bond, a process that is unlikely to occur directly even with the help of an unsaturated metal center. Instead, the process is likely to involve Si–C bond cleavage and formation via oxidative additions and reductive eliminations, respectively, as such steps have been found to be facile in $\kappa P,P,Si$ pincer complexes of Ni, Pd, Rh, and Ir.^{27,28,31} In any case, regardless of the details of each structure, the reactions of Scheme 5 show that the inserted carbenes can indeed participate in reactions typical of alkyls such as migratory insertions and reductive eliminations.

CONCLUSIONS

The $\kappa P,P,Si$ pincer ligand [Si(Me)(C₆H₄-2-PiPr₂)₂] permits the preparation of five-coordinate ruthenium carbene complexes isoelectronic with the Grubbs catalyst but not isostructural, as they can offer a coordination site *cis* to the carbene ligand. The reactions with a variety of incoming ligands and other reagents indicate that the first response of these complexes to an increase of the coordination number around the metal is the insertion of the carbene ligand into the Ru–Si bond. Such an insertion generates an alkyl moiety as well as a new coordination vacancy that enables further reactions. Since the insertion is reversible, these reactions can be those typical of carbene ligands, such as C–H bond functionalizations and ketene formation from CO. Alternatively, they can be those characteristic of metal-bound alkyls, such as C–H reductive eliminations and alkyne insertions. Ultimately, this capability of the pincer contributes to improve and diversify the reactivity of carbene ligands and therefore might constitute an exploitable ligand resource. Our current research efforts aim to recognize transformations that can benefit from this resource and to extend it to chemical entities other than carbenes.

ASSOCIATED CONTENT

Supporting Information

Text, figures, and CIF files giving experimental details for compound syntheses, characterization data, and full crystallographic descriptions. This material is available free of charge via the Internet at <http://pubs.acs.org>.

AUTHOR INFORMATION

Corresponding Author

martam@unizar.es; sola@unizar.es

Notes

The authors declare no competing financial interest.

ACKNOWLEDGMENTS

This research was supported by the Spanish MINECO (Grants CTQ2009-08023 and CTQ2012-31774) and CSIC (Grant PIE 201280E109).

REFERENCES

- (1) (a) Hindson, K.; de Bruin, B. *Eur. J. Inorg. Chem.* **2012**, 340. (b) Kaim, W. *Inorg. Chem.* **2011**, *50*, 9752. (c) Grützmacher, H. *Angew. Chem., Int. Ed.* **2008**, *47*, 1814. (d) Crabtree, R. H. *New J. Chem.* **2011**, *35*, 18. (e) Luca, O. R.; Crabtree, R. H. *Chem. Soc. Rev.* **2013**, *42*, 1440. (f) Lyaskovskyy, V.; de Bruin, B. *ACS Catal.* **2012**, *2*, 270. (g) Dzik, W. I.; van der Vlugt, J. I.; Reek, J. N. H.; de Bruin, B. *Angew. Chem., Int. Ed.* **2011**, *50*, 3356. (h) Chirik, P. J.; Wieghardt, K. *Science* **2010**, *327*, 794. (i) Annibale, V. T.; Song, D. *RSC Adv.* **2013**, *3*, 11432. (j) Askevold, B.; Roesky, H. W.; Schneider, S. *ChemCatChem* **2012**, *4*, 307. (k) Gunanathan, C.; Milstein, D. *Acc. Chem. Res.* **2011**, *44*, 588. (l) Ikariya, T. *Bull. Chem. Soc. Jpn.* **2011**, *84*, 1. (m) For leading references of bifunctional ligands that exploit supramolecular interactions see ref 3 and: (a) Dydio, P.; Detz, R. J.; Reek, J. N. H. *J. Am. Chem. Soc.* **2013**, *135*, 10817. (b) Fackler, P.; Huber, S. M.; Bach, T. *J. Am. Chem. Soc.* **2012**, *134*, 12869. (n) (a) Kaim, W.; Schwederski, B. *Coord. Chem. Rev.* **2010**, *254*, 1580. (b) Buckel, W. *Angew. Chem., Int. Ed.* **2009**, *48*, 6779. (c) Stubbe, J.; Nocera, D. G.; Yee, C. S.; Chang, M. C. Y. *Chem. Rev.* **2003**, *103*, 2167. (d) Whittaker, J. W. *Chem. Rev.* **2003**, *103*, 2347. (e) Stubbe, J.; van der Donk, W. A. *Chem. Rev.* **1998**, *98*, 705. (o) (a) Milstein, D. *Top. Catal.* **2010**, *53*, 915. (b) Ikariya, T.; Blacker, A. J. *Acc. Chem. Res.* **2007**, *40*, 1300. (c) Conley, B. L.; Pennington-Boggio, M. K.; Boz, E.; Williams, T. J. *Chem. Rev.* **2010**, *110*, 2294. (d) Käß, M.; Friedrich, A.; Drees, M.; Schneider, S. *Angew. Chem., Int. Ed.* **2009**, *48*, 905. (e) Noyori, R.; Yamakawa, M.; Hashiguchi, S. *J. Org. Chem.* **2001**, *66*, 7931. (f) Dang, Y.; Qu, S.; Wang, Z.-X.; Wang, X. *Organometallics* **2013**, *32*, 2804. (p) (a) Kohl, S. W.; Weiner, L.; Schwartsburd, L.; Konstantinovski, L.; Shimon, L. J. W.; Ben-David, Y.; Iron, M. A.; Milstein, D. *Science* **2009**, *324*, 74. (b) Hettler, D. G. H.; van der Vlugt, J. I.; de Bruin, B.; Reek, J. N. H. *Angew. Chem., Int. Ed.* **2009**, *48*, 8178. (c) Ackermann, J. *Chem. Rev.* **2011**, *111*, 1315. (q) Sola, E.; García-Camprubí, A.; Andrés, J. L.; Martín, M.; Plou, P. *J. Am. Chem. Soc.* **2010**, *132*, 9111. (r) For recent work in silyl-pincer complexes and leading references: (a) Kirai, N.; Takaya, J.; Iwasawa, N. *J. Am. Chem. Soc.* **2013**, *135*, 2493. (b) Wu, S.; Li, X.; Xiong, Z.; Xu, W.; Lu, Y.; Sun, H. *Organometallics* **2013**, *32*, 3227. (c) Joost, M.; Mallet-Ladeira, S.; Miqueu, K.; Amgoune, A.; Bourissou, D. *Organometallics* **2013**, *32*, 898. (d) Mitton, S. J.; Turculet, L. *Chem. Eur. J.* **2012**, *18*, 15258. (e) Fang, H.; Choe, Y.-K.; Li, Y.; Shimada, S. *Chem. Asian J.* **2011**, *6*, 2512. (f) Yang, J.; Del Rosal, I.; Fasulo, M.; Sangtrirutnugul, P.; Maron, L.; Tilley, T. D. *Organometallics* **2010**, *29*, 5544. (g) Zhou, X.; Stobart, S. R. *Organometallics* **2001**, *20*, 1898. See also: (h) Montiel-Palma, V.; Muñoz-Hernández, M. A.; Cuevas-Chávez, C. A.; Vendier, L.; Grellier, M.; Sabo-Etienne, S. *Inorg. Chem.* **2013**, *52*, 9798. (i) Brück, A.; Gallego, D.; Wang, W.; Irran, E.; Driess, M.; Hartwig, J. F. *Angew. Chem., Int. Ed.* **2012**, *51*, 11478. (s) (a) Schwab, P.; Grubbs, R. H.; Ziller, J. W. *J. Am. Chem. Soc.* **1996**, *118*, 100. (b) Love, J. A.; Sanford, M. S.; Day, M. W.; Grubbs, R. H. *J. Am. Chem. Soc.* **2003**, *125*, 10103. (t) For leading references on the mechanism of olefin metathesis: Ashworth, I. W.; Hillier, I. H.; Nelson, D. J.; Percy, J. M.; Vincent, M. A. *ACS Catal.* **2013**, *3*, 1929. (u) MacInnis, M. C.; McDonald, R.; Ferguson, M. J.; Tobisch, S.; Turculet, L. *J. Am. Chem. Soc.* **2011**, *133*, 13622. (v) (a) Katayama, H.; Yari, H.; Tanaka, M.; Ozawa, F. *Chem. Commun.* **2005**, 4336. See also: (b) Lee, J.-H.; Cauton, K. G. *J. Organomet. Chem.* **2008**, *693*, 1664. (c) Bassetti, M.; Marini, S.; Gamasa, M. P.; Rodríguez-Álvarez, Y.; García-Granda, S. *Organometallics* **2002**, *21*, 4815. (16) Katayama, H.; Ozawa, F. *Organometallics* **1998**, *17*, 5190. (17) Wolf, J.; Stuer, W.; Grunwald, C.; Gevert, O.; Laubender, M.; Werner, H. *Eur. J. Inorg. Chem.* **1998**, 1827. (18) Coe, B. J.; Glenwright, S. J. *Coord. Chem. Rev.* **2000**, *203*, 5. (19) Yamaguchi, M.; Arikawa, Y.; Nishimura, Y.; Umakoshi, K.; Onishi, M. *Chem. Commun.* **2009**, 2911. (20) Ritter, T.; Hejl, A.; Wenzel, A. G.; Funk, T. W.; Grubbs, R. H. *Organometallics* **2006**, *25*, 5740. (21) (a) Allen, A. D.; Egle, I.; Janoschek, R.; Liu, H. W.; Ma, J.; Marra, R.; Tidwell, T. T. *Chem. Lett.* **1996**, 45. (b) Valentí, E.; Pericás, M. A.; Serratos, F. J. *Org. Chem.* **1990**, *55*, 395. (c) Black, T. H.; Farrell, J. R.; Probst, D. A.; Zoltz, M. C. *Synth. Commun.* **2002**, *32*, 2083. (22) For precedents of catalytic formation of ketenes: (a) Paul, N. D.; Chirila, A.; Lu, H.; Zhang, X. P.; de Bruin, B. *Chem. Eur. J.* **2013**, *19*, 12953. (b) Zhang, Z.; Liu, Y.; Ling, L.; Li, Y.; Dong, Y.; Gong, M.; Zhao, X.; Zhang, Y.; Wang, J. *J. Am. Chem. Soc.* **2011**, *133*, 4330. (23) For leading references on metal-bound carbene insertions: Franssen, N. M. G.; Walters, A. J. C.; Reek, J. N. H.; de Bruin, B. *Catal. Sci. Technol.* **2011**, *1*, 153. (24) For carbene migratory insertions in related complexes: (a) Burrell, A. K.; Clark, G. R.; Rickard, C. E. F.; Roper, W. R.; Wright, A. H. *J. Chem. Soc., Dalton Trans.* **1991**, 609. See also: (b) Hill, A. F.; Roper, W. R.; Waters, J. M.; Wright, A. H. *J. Am. Chem. Soc.* **1983**, *105*, 5939. (c) Galan, B. R.; Pitak, M.; Gembicky, M.; Keister, J. B.; Diver, S. T. *J. Am. Chem. Soc.* **2009**, *131*, 6822. (25) Latos-Grazynski, L.; Cheng, R.-J.; La Mar, G. N.; Balch, A. L. *J. Am. Chem. Soc.* **1981**, *103*, 4270. (26) Whited, M. T.; Grubbs, R. H. *Organometallics* **2008**, *27*, 5737. (27) (a) Mitton, S. J.; McDonald, R.; Turculet, L. *Angew. Chem., Int. Ed.* **2009**, *48*, 8568. (b) Mitton, S. J.; McDonald, R.; Turculet, L. *Polyhedron* **2013**, *52*, 750. (c) Kameo, H.; Ishii, S.; Nakazawa, H. *Dalton Trans.* **2013**, 42, 4663. (28) García-Camprubí, A.; Martín, M.; Sola, E. *Inorg. Chem.* **2010**, *49*, 10649. (29) Stobart, S. R.; Zhou, X.; Cea-Olivares, R.; Toscazo, A. *Organometallics* **2001**, *20*, 4766. (30) For leading references: (a) Montag, M.; Efremenko, I.; Diskin-Posner, Y.; Ben-David, Y.; Martin, J. M. L.; Milstein, D. *Organometallics* **2012**, *31*, 505. See also: (b) Steinke, T.; Shaw, B. K.; Jong, H.; Patrick, B. O.; Fryzuk, M. D.; Green, J. C. *J. Am. Chem. Soc.* **2009**, *131*, 10461. (31) (a) Takaya, J.; Iwasawa, N. *Organometallics* **2009**, *28*, 6636. (b) Takaya, J.; Iwasawa, N. *J. Am. Chem. Soc.* **2008**, *130*, 15254. See also: (c) North, M. *Angew. Chem., Int. Ed.* **2009**, *48*, 4104. (32) Doyle, M. P.; Duffy, R.; Ratnikov, M.; Zhou, L. *Chem. Rev.* **2010**, *110*, 704. (33) Díaz-Requejo, M. M.; Pérez, P. J. *Chem. Rev.* **2008**, *108*, 3379. (34) Lo, V. K.-Y.; Guo, Z.; Choi, M. K.-W.; Yu, W.-Y.; Huang, J.-S.; Che, C.-M. *J. Am. Chem. Soc.* **2012**, *134*, 7588. (35) (a) Trnka, T. M.; Day, M. W.; Grubbs, R. H. *Organometallics* **2001**, *20*, 3845. (b) O'Connor, J. M.; Baldrige, K. K.; Vélez, C. L.; Rheingold, A. L.; Moore, C. E. *J. Am. Chem. Soc.* **2013**, *135*, 8826 and references therein. See also: (c) Le Pailh, J.; Vovard-Le Bray, C.; Dérien, S.; Dixneuf, P. H. *J. Am. Chem. Soc.* **2010**, *132*, 7391. (36) For leading references on alkyne insertions into M–C bonds, see: Li, L.; Jiao, Y.; Brennessel, W. W.; Jones, W. D. *Organometallics* **2010**, *29*, 4593. (37) For an example of 1,3-hydrogen migration, see: (a) MacDougall, T. J.; Samant, R. G.; Trepanier, S. J.; Ferguson, M. J.; McDonald, R.; Cowie, M. *Organometallics* **2012**, *31*, 1857. For related isomerizations of hydrocarbyl ligands leading to allyls, see: (b) Esteruelas, M. A.; Lahoz, F. J.; Oñate, E.; Oro, L. A.; Sola, E. *J. Am. Chem. Soc.* **1996**, *118*, 89. (38) Frohnapfel, D. S.; Templeton, J. L. *Coord. Chem. Rev.* **2000**, *206–207*, 199.

(39) Imazaki, Y.; Shirakawa, E.; Ueno, R.; Hayashi, T. *J. Am. Chem. Soc.* **2012**, *134*, 14760.

(40) (a) Crabtree, R. H. *New J. Chem.* **2003**, *27*, 771. (b) Chung, L. W.; Wu, Y.-D.; Trost, B. M.; Ball, Z. T. *J. Am. Chem. Soc.* **2003**, *125*, 11578.